

Repurposing of Statins Against Superficial Fungal Infections

Sarita¹, Neha Mathur^{1*}, Pooja Chawla², Manish Mathur³

¹Amity Institute Pharmacy, Lucknow, Amity University Uttar Pradesh, Sector 125, Noida, 201313, India, nmathur1@amity.edu;neha07

²Baba Farid University of Health Sciences Faridkot Punjab, 151203, India, pvchawla@gmail.com

³Department of Academic Affairs, Amity University Uttar Pradesh, Lucknow campus, mathur.man7@gmail.com

*Corresponding author: Neha Mathur

KEYWORDS

Repurposing, Azoles, Resistance, Infections.

ABSTRACT

In a few decades fungal infections will become a major worldwide health concern. Research reveal that the fungal strain becomes resistant to current medications in cases of HIV infections, corona infections and environmental factors particularly in people with impaired immune systems. The amount of organ transplants and medication used for therapy all have contributed to an increase in the immunocompromised population. The fungal infections are becoming a more significant cause of mortality and morbidity. An estimated 1.5 million fatal consequences are caused by fungal pathogens annually. In a few decades, fungal infections will become a major worldwide health concern, so that unprecedented rates of fungal resistance to currently available antifungal medicines has been observed.

The drug repurposing approaches lowers costs and time by investigating previously approved medicines with known safety and pharmacokinetics toxicity profile for novel therapeutic effects.

The HMG – CoA reductase inhibitors drugs statins shows antifungal properties against tinea spp. group of common fungus that causes superficial infections. We have evaluated statins for their antifungal potential by insilico studies & Invitro studies & validate results with standard drugs itraconazole & ketoconazole. The docking studies shows highest binding energy shown by atorvastatin among all statin

were used for docking studies pravastatin , atorvastatin, simvastatin ,fluvastatin & rosuvastatin . against fungal protein (PDB ID:5V5Z) & human protein (PDB ID: 3LD6) was found to be -13.52 &13.4 kcal/mole .The invitro studies shows MIC values for atorvastatin against Trichophyton rubrum , Microsporum canis & Epidermatophyton floccosum fungal strains found between 125 µg/ml to 150 125 µg/ml where as for standard drugs was found between 12.5 µg/ml to 25 µg/ml. Following insilico & invitro research atorvastatin determined and may be used for the treatment of fungal infections.

1. Introduction and Background

The growth of fungi that gain resistance is currently exceeding the slow process of developing new antifungals. Further delays are added by the rigorous process of identifying new compounds and the extended method for finding new, effective antifungals (Fisher, Hawkins, Sanglard, & Gurr, 2018). Only three groups of antifungal medications—azoles, echinocandins, and polyenes are available to combat systemic fungal infections because to a lack of therapeutic options (Revie, Iyer, Robbins, & Cowen, 2018). Fungi have acquired remarkable resistance to currently available antifungal medicines. Among the causes are environmental causes for antifungal resistance (Sanglard, 2016). The development of novel antifungals is a laborious process that is currently overtaken by the rapid rise of fungi that develop resistance. Azoles are widely used in animal health care, crop protection, and the lumber and paint industries. Further delays are exacerbated by the laborious procedure of registering new compounds and the delayed process of finding new, effective antifungals (Fisher, Hawkins, Sanglard, & Gurr, 2018). The hydroxyl methyl glutaryl CoA (HMG-CoA) reductase enzyme is inhibited by statins. By blocking a crucial stage in the biosynthesis of sterols, They have emerged as a major medication for lowering the risk of cardiovascular disease (Oesterle, Laufs, & Liao, 2017), despite the advent of new lipid-modifying drugs (Banach et al., 2015; Sahebkar & Watts, 2013). Furthermore, a number of lipid-independent pleiotropic actions have been identified for statins (Chruściel et al., 2016; Parizadeh et al., 2011; Sahebkar, Kotani, et al., 2015; Sahebkar, Serban, et al., 2015; Sahebkar et al., 2016). The use of statins has also been linked to better outcomes for those with morbidities irrelevant to cardiovascular disease, such as rheumatoid arthritis, certain types of cancer, and chronic obstructive pulmonary disease (He et al., 2018). 200 million individuals worldwide currently take statins . Since they are strong competitive inhibitors of HMG Co A reductase (3-hydroxy methylglutaryl coenzyme), statins have been used as cholesterol-lowering medications. The enzyme that regulates the rate of the cholesterol biosynthesis pathway in both humans and fungus is called HMG Co reductase. The fungal cell wall that contains ergosterol at the initial stages of its manufacture

2. Material and Methods

2.1. Docking studies

To achieve molecular docking, X-ESS (Multi Target Multi Ligand Enhanced Sampling Screening) was used. SDF files were used as ligand input, and the target proteins were extracted straight from BioIn in pdb format. The number of binding sites' amino acid residues was specified in order to carry out active site docking. To obtain statistically better data, the Lamarckian genetic algorithm (LGA) was utilized for docking, using 100 GA runs.

2.1.1. Selection of desired protein

The Protein Data Bank (PDB) offered the desired protein. The three-dimensional (3D) structures of the human "Lanosterol 14 - alpha demethylase" proteins are available as PDBs: 3JUS, 3UV, 3LD6, 4UHI, and 4UHL. Their PDB ID is 3LD6 (Uniport ID: Q1680). The human lanosterol 14-demethylase (CYP51) crystal structure complexed with ketoconazole, whereas the fungal "Lanosterol 14-alpha demethylase" proteins had 3D structures with PDB ID: 5v5z (Uniport ID: P10613) and reported resolutions of 2.90 Å for 5v5z protein and 2.80 Å for 3LD6 protein. With the aid of the software version PRinS3 (Prescience in silico Solution Suite), the 3D structure of the protein templet was confirmed.

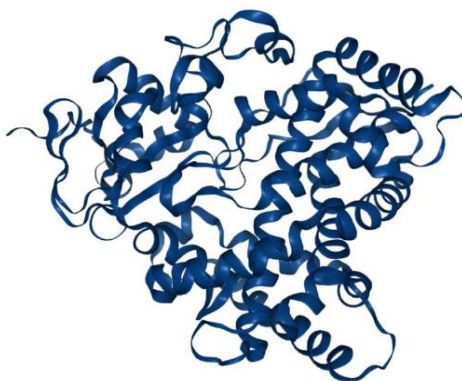


Figure (1) : 3D structure of Human Lanosterol 14 - alpha demethylase (PDB ID: 3LD6).

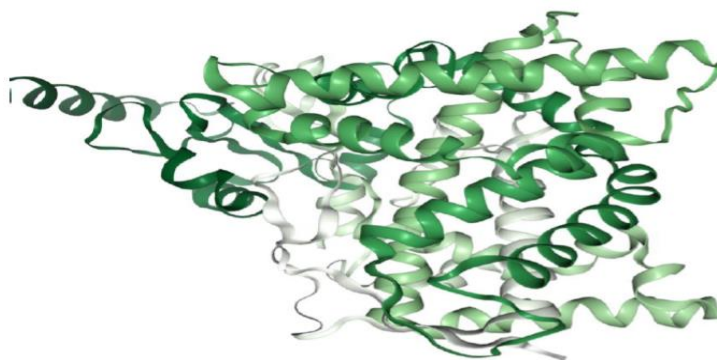


Figure (2) : 3D structure of Fungal Lanosterol 14 - alpha demethylase (PDB ID: 5V5Z)

2.1.2. Selection of ligands

In the initial stages of ergosterol biosynthesis during the manufacture of 3-hydroxy-3-methylglutaryl (HMG), the fungal cell wall is composed of ergosterol.- CoA from three molecules of acetylcholine, followed by (HMG) HMG-CoA reductase catalyzes the formation of CoA, and statins block this enzyme, which is necessary for the synthesis of ergosterol. Statins are employed for their possible antifungal properties since 14-alpha lanosterol demethylase is an essential enzyme needed for fungus to synthesize ergosterol . As indicated in Table-1, the ligands were gathered and stored in sdf format using the PubChem database using the PRinS3 (Prescience in silico Solution Suite) software version, these molecules were ready for docking.

Table (1) : List of Ligands used against desired protein

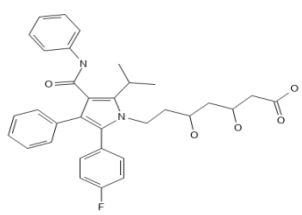
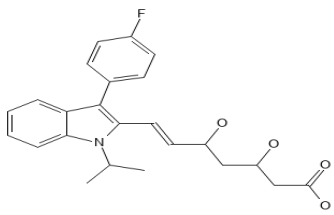
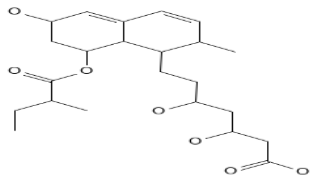
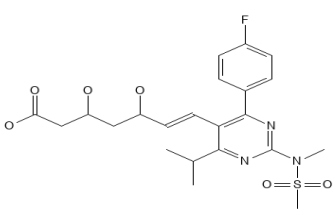
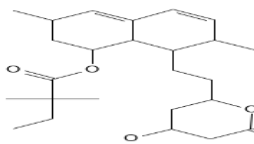
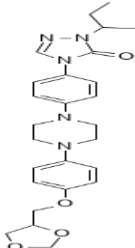
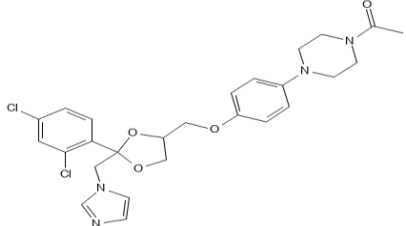
S.No.	Ligand name	PubChem ID	Molecular formula & Molecular weight	Chemical structure
1.	Atorvastatin	Compound CID: 60823	C ₃₃ H ₃₅ FN ₂ O ₅ MW: 558.6g/mol	
2.	Fluvastatin	Compound CID: 446155	C ₂₄ H ₂₆ FN ₂ O ₄ MW: 411.5g/mol	
3.	Pravastatin	Compound CID: 54687	C ₂₃ H ₃₆ O ₇ MW: 424.5g/mol	
4.	Rosuvastatin	Compound CID: 446157	C ₂₂ H ₂₈ FN ₃ O ₆ S MW: 481.5g/mol	
5.	Simvastatin	Compound CID: 54454	C ₂₅ H ₃₈ O ₅ MW: 418.6g/mol	

Table (2): List of Standard drugs used against desired protein

S.No.	Ligand name	PubChem ID	Molecular formula & Molecular weight	Chemical structure
1.	Itraconazole	Compound CID: 55283	C ₃₅ H ₃₈ Cl ₂ N ₈ O ₄ MW: 705.6g/mol	
2.	Ketoconazole	Compound CID: 456201	C ₂₆ H ₂₈ Cl ₂ N ₄ O ₄ MW: 531.4g/mol	

2.1.3. Preparation of protein

Proteins were ready for binding using the BioIn program from PRinS3 (Prescience insilico Solution Suite). BioIn was used for procedures like adding hydrogen atoms, refining of loops, removal of water molecules, and addition of protein residues that were absent. The protein was obtained as a PDB file download.

2.1.4. Binding sites prediction

Literature was used to identify the binding locations. Researchers have found binding sites for 3LD6 in two investigations, with methylphloroglucinal derivatives (Ye et al., 2018) and epifriedelanol (Ramadhani, 2020) as the ligands, respectively. *Guazuma ulmifolia* is the natural source of epifriedelanol, and phloroglucinols have shown strong antifungal effects. The binding sites for 3LD6 were determined to be 379Ile, 378Met, 487Met, 131Tyr, 135Thr, 134Leu, and 382Arg taken together. Similarly, coumarin derivatives (Paul Andrei & Georgeta, 2021) and 3-sitosterol hydrogen phthalate (Khan et al., 2020), a possible antifungal drug, are the ligands that have been investigated for 5V5Z. The 5V5Z fungal Lanosterol 14 alpha demethylases research study revealed the following binding sites: 380Phe, 118Tyr, 508, 304Ile, 131Ile, 132Tyr, 139Leu, 150Leu, 471Ile, 476Ala, 475Phe, and 143Lys.

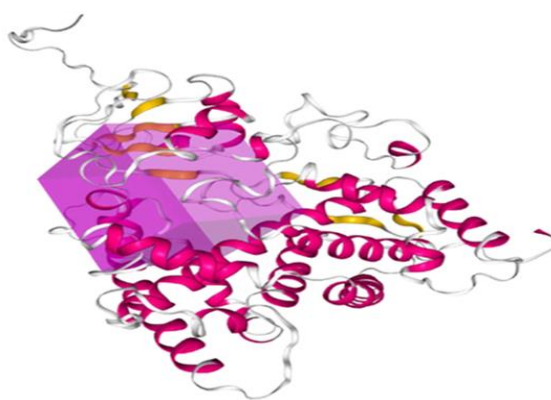


Figure (3): Binding sites of 3LD6 inside grid box

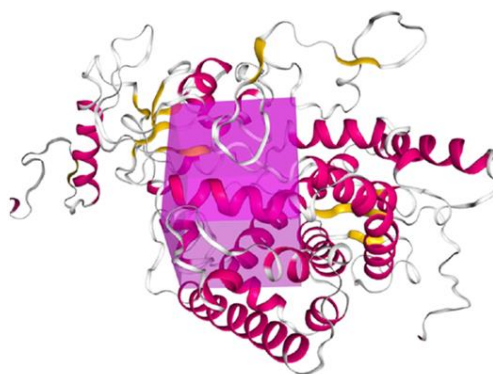


Figure (4) : Binding sites of 5V5Z inside grid box

2.1.5. Interactions between ligands and proteins

X-ESS (Multi Ligand Enhanced Sample screening) was used to optimize the ligands and proteins. The target proteins were extracted in PDB format from the protein data library, and SDF files were used as ligand input. By defining the number of amino acid residues in the binding locations, active site docking was carried out. To get statistically superior data for the docking procedure, 100 GA runs were combined with the Lamarckian genetic algorithm (LGA).

2.2. Molecular dynamics (MD) Simulation studies

In our study, the lowest binding energy was taken into consideration for a molecular dynamics (MD) simulation, which is used to predict the binding poses and binding affinities of small molecules with the target proteins. It is also useful for evaluating the stability of the binding and any conformational changes in ligands during binding with proteins. Simulations were conducted using the PRinS3 X-ESS program. The protein and ligand

systems. The ligand force field was created using the CHARMM27 force field from the SwissParam web server (<https://www.swissparam.ch/>). The X-ESS application was provided the mol2 and itp files. The force field for the protein was chosen to be CHARMM27. In order to fill the unit cell, the TIP3P water model was chosen, and water molecules were incorporated into the topology and structure files. This is accomplished in two stages: equilibration is done with an NVT ensemble first, followed by an NPT ensemble. The NPT ensemble requires the preservation of constant volume, temperature, and particle count because, in contrast to the NVT ensemble, it maintains constant temperature, pressure, and particle count. Another name for the NVT ensemble is the isothermal-isochoric ensemble, while another name for the NPT ensemble is the isothermal-isobaric ensemble. Both NVT and NPT ensembles are used in the simulation procedure for this application in order to attain system equilibration. The simulation times for NPT and NVT were set at 0.1 and 10 ns, respectively. 3LD6's binding energy varied between -11.11 and -13.52 kcal/mol. For 5V5Z, this range was -11.48 to -13.49. The binding energy range is constrained because this group consists of only five compounds. Pravastatin and atorvastatin had the greatest docking energy values for the protein 5V5Z. In the instance of 3LD6, the drugs with the highest docking energies were atorvastatin and fluvastatin.

Table (3): Binding energy & amino acid residues of statin and standard drugs against two protein targets.

Proteins	Compound	Binding energy (kal/mol)	Amino acid residue
3LD6	Atorvastatin	-13.49	236HIS
	Fluvastatin	-12.12	376PRO, 378MET, 379ILE
5V5Z	Pravastatin	-12.43	132TYR, 303GLY, 307GLY
	Atorvastatin	-13.52	143LYS, 468HIS
Standard drugs			
3LD6	Ketoconazole	-11.53	489 HIS
	Itraconazole	-14.25	135 THR, 378MET
5V5Z	Ketoconazole	-11.19	143 LYS, 132TYR
	Itraconazole	-11.79	132 TYR

3. In Vitro Studies

A drug sample and fungal strain *Trichophyton rubrum* (MTCC ID: 3272), *Microsporum canis* (MTCC ID: 3270) & *Epidermatophyton floccosum* (MTCC ID: 7880) were obtained from the Microbial Type Culture collection in order to assess antidermatophytic activity. The fungal strains were incubated at 28 °C while being grown on Sabouraud dextrose agar media (Difco, BD Biosciences). The drug sample were procured from, atorvastatin (Reine Life science MFG & EXP: Bulk & Drugs intermediates) and the standard drugs ketoconazole (Arti Drugs Limited Manufacturer of Bulk Drugs & Chemicals) and itraconazole (Metro chem API private limited, Sunder Nagar, Hyderabad) were assessed.

3.1. Antifungal sensitivity test (AST)

The antifungal sensitivity test was performed to determine the given sample's sensitivity towards the given sample atorvastatin shows the zone of inhibition against three fungal strain *Trichophyton rubrum*, *E. floccosum* & *Microsporum canis* tested against three concentrations of atorvastatin the zone of inhibition summarized shown in the table [9] & Figure 18, 19 & 20. The Disc Diffusion Method was used to assess the activity. The culture media supplied by Hi-media, which involves dissolving 38 g of the Muller-Hinton Agar (MHA) medium in 1 liter of water, the medium was prepared. After that, the media is autoclaved for 15 minutes at 121°C and 15 psi using an autoclave (Gentek India Pvt. Ltd.). The culture media (20 milliliters each plate) were transferred using aseptic techniques into sterile glass Petri dishes that were placed in a laminar airflow after the sterilization process (Toshiba, India). The plates were allowed to set in laminar, and then a fungal culture dressed in LB liquid broth was introduced into the media. A sterilized glass rod was utilized to distribute 100µl of the culture broth uniformly throughout the media. After spreading for ten minutes, the discs were placed into the medium plates using sterile forceps. The plates were paraffin-sealed and incubated at 37°C for 24 and 48 hours after the samples had taken up the medium. Itraconazole and ketoconazole at 300 ppm concentrations were utilized as positive controls on two of the discs, DMSO was used as a negative control on one disk, and three discs contained different concentrations of the provided material. The fourth day of inhibition was used to monitor the clear zone around the well, which is referred to as the zone of inhibition. The diameter of each of these zones was measured in millimeters.

3.1.1. Minimum Inhibitory Concentration (MIC)

To find the samples' lowest inhibitory concentration, Sabouraud dextrose broth was utilized. Standard composition was used to make the broth, and autoclaving was used to sterilize it. The experiment employed ten test tubes, arranged from highest to lowest in decreasing order of drug concentration, as well as media control (containing broth and no test organism) and growth control (containing test organism and no test material). Then, 100µl of a fungal culture of the strain under study that had been cultivating for a full day was added to each tube containing the use and test sample. Following the addition of the fungal culture, the tubes were sealed and incubated for 48 hours at 25°C. The turbidity in the medium, a sign of fungal growth, was checked in the tubes using a UV-Visible Double Beam Spectrophotometer (PC-Based Double Beam UV-VIS Spectrophotometer 2201). The optical density of each tube was measured, and the MIC value for this set of analyses is determined by determining the minimum concentration of the antifungal drug at which no turbidity is detectable. The tubes were sealed and left to incubate at 25°C for 48 hours after the fungal culture was added. Turbidity in the media, an indicator of fungal growth, was examined in the tubes after incubation. Each tube's optical density was measured using a UV-Visible Double Beam Spectrophotometer (PC-Based Double Beam UV-VIS Spectrophotometer 2021). Finding the lowest concentration of the antifungal drug at which no detectable turbidity occurs yields the MIC value for this series of analyses. The tubes showing no turbidity were then spread on sabouraud dextrose agar plates to determine the Minimum fungicidal concentrations. Plates with no colony appearance were recorded as the Minimum fungicidal concentrations.

4. Results

4.1. Molecular docking & MD simulation studies

Statins were chosen for molecular docking and additional MD simulation studies based on the synthetic pathway of fungal cell wall. Two protein targets were selected the fungal protein lanosterol 14-alpha-demethylase (PDB ID: 5V5Z) and the human protein lanosterol 14-alpha-demethylase (PDB ID: 3LD6). Each compound produces a collection of nine top-scoring docked poses in molecular docking calculations. The binding energy and amino acid residues of anticonvulsant and conventional medications against two protein targets are highlighted in Table No. 3.

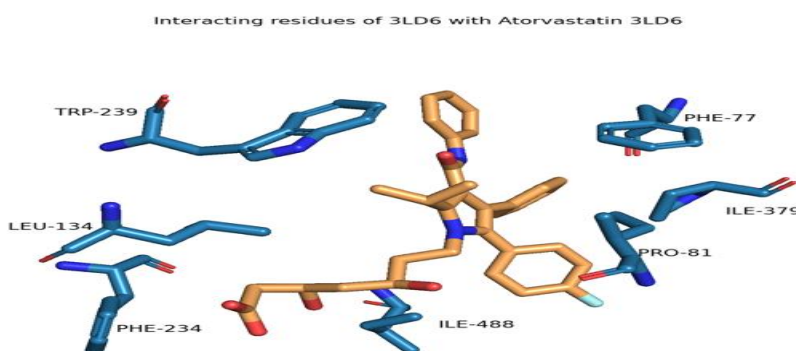


Figure (5): Interaction of Atorvastatin with 3LD6

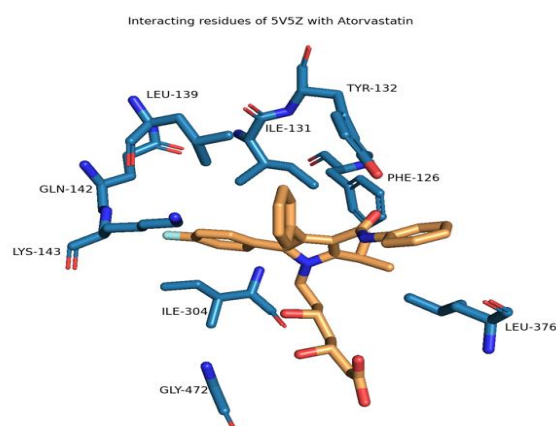


Figure (6) : Interaction of Atorvastatin with 5V5Z

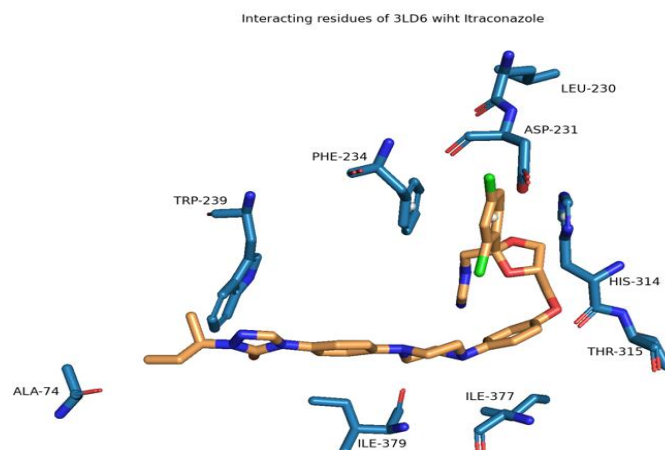


Figure (7) : Interaction of Itraconazole with 3LD6

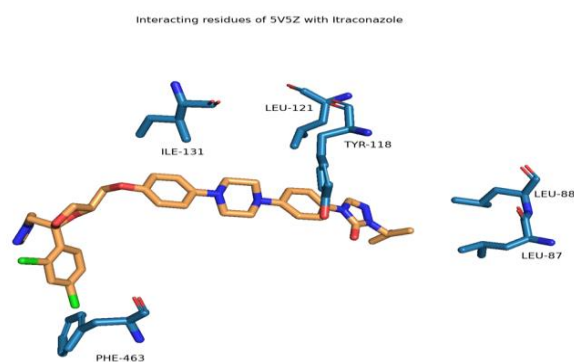


Figure (8) : Interaction of Itraconazole with 5V5Z

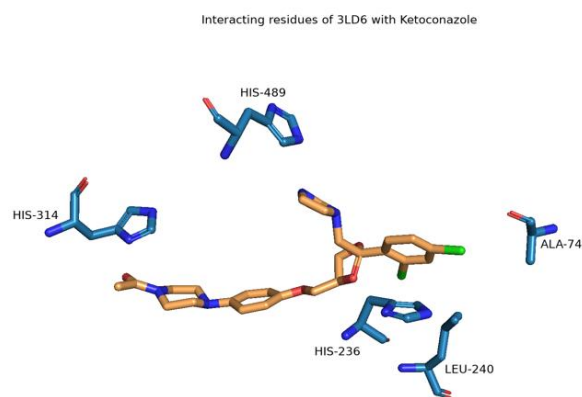


Figure (9) : Interaction of Ketoconazole with 3LD6

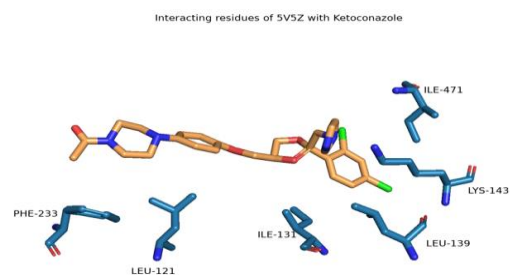


Figure (10) : Interaction of Ketoconazole with 5V5Z

Table (4): Binding energy & amino acid residues of statin and standard drugs against two protein targets

Proteins	Compound	Binding energy(kcal/mol)	Amino acid residue
3LD6	Atorvastatin	-13.49	236His
	Fluvastatin	-12.12	376Pro, 378Met, 379Ile
5V5Z	Pravastatin	-12.43	132Tyr, 303Gly, 307Gly
	Atorvastatin	-13.52	143Lys, 468His
Standard drugs			
3LD6	Ketoconazole	-11.88	379 Ty
	Itraconazole	-14.07	-
5V5Z	Ketoconazole	-11.24	-
	Itraconazole	-12.24	132Tyr, 377His,378 Ser

3LD6's binding energy varied between -13.44 to 12.58 kcal/mol. for 5V5Z, this range was – 12.05 to - 13.01kcal/mol. The binding energy range is constrained because this group consists of only five compounds. Pravastatin and atorvastatin had the greatest docking energy values for the protein 5V5Z. In the instance of 3LD6, the drugs with the highest docking energies were atorvastatin and fluvastatin.

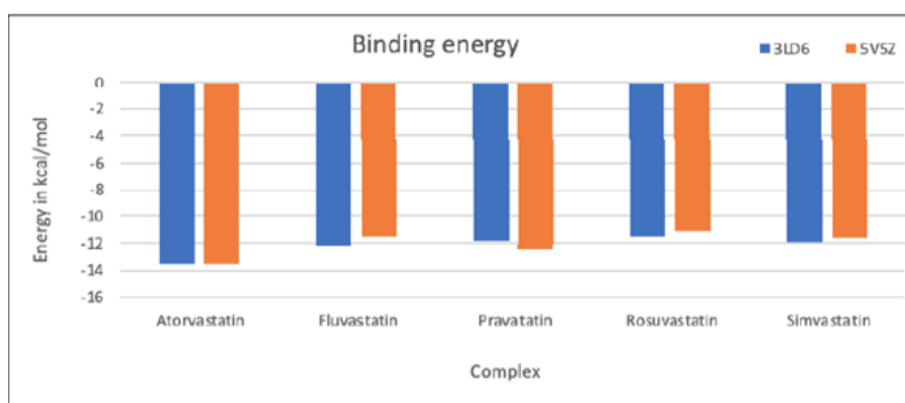


Figure (11) : Graphical representation of binding energy

4.1.1. Average RMSD (nm)

The RMSD (Root Square Mean Deviation) encapsulates the stability of the refined structure by displaying various fluctuations present in the complex during the MDS. The target's binding pocket residues' Root Mean Square Deviation (RMSD) is computed by contrasting the MD equilibrated structure—the final frame of the MD simulation with the original MD configuration. The results are shown in the RMSD vs ligand graph in Figure 6 and for standard drugs in Figure 7.

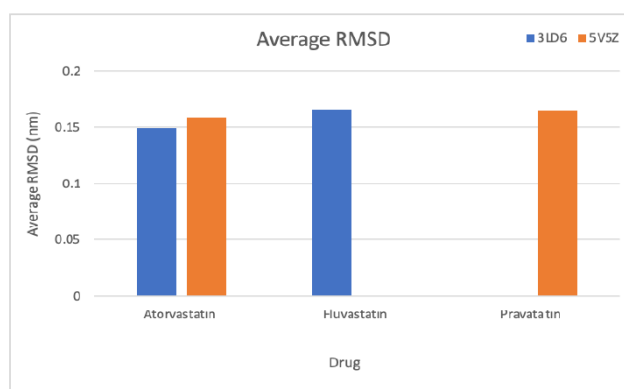


Figure (12) : Graph of average RMSD (nm) values for statins against 3LD6 and 5V5Z Proteins

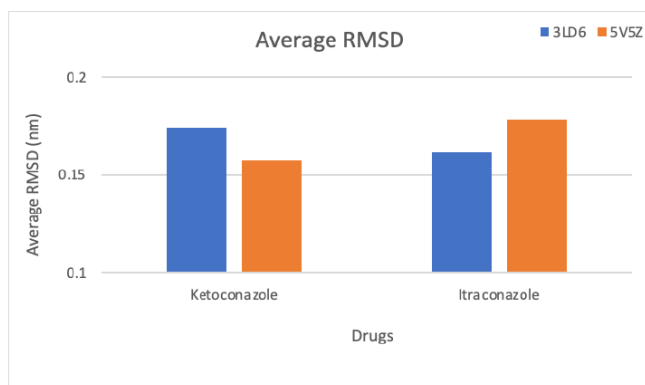


Figure (13) : Graph of average RMSD (nm) values for standard drugs against 3LD6 and 5V5Z Proteins

4.1.2. Hydrogen Bonds

The number of hydrogen bonds between the ligand and the target is shown on the graph. The requirements of bond length 0.35 nm and angle 30° are used to calculate these hydrogen bonds. As seen in Figure 8, all of the complexes include hydrogen bonds between one and three.

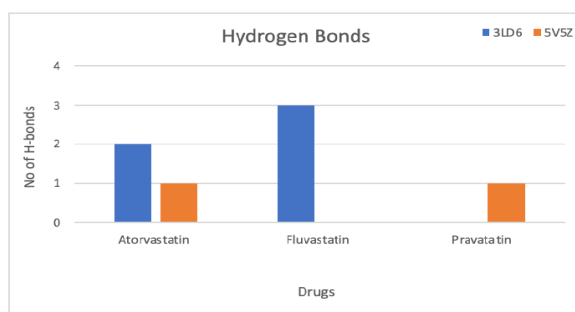


Figure (14) : Graph showing the number of hydrogen bonds between the ligand and the target protein (3LD6 and 5V5Z) of statin drugs.

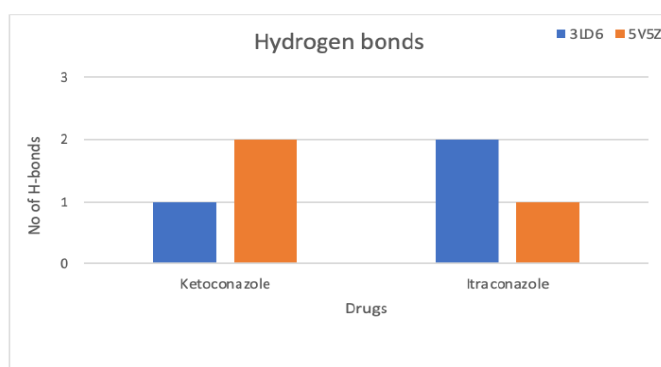


Figure (15): Graph showing the number of hydrogen bonds between the ligand and the target protein (3LD6 and 5V5Z) of standard drugs

4.1.3. Interaction Energy

The interaction energies between ligands and proteins, known as the non-bonded ones, (the van der Waals and Coulomb interactions) are determined and depicted in figure 9. This gives an idea about the strength of interaction between protein and ligand. for proteins with PDBID 3LD6 & 5V5Z, atorvastatin displayed favourable results.

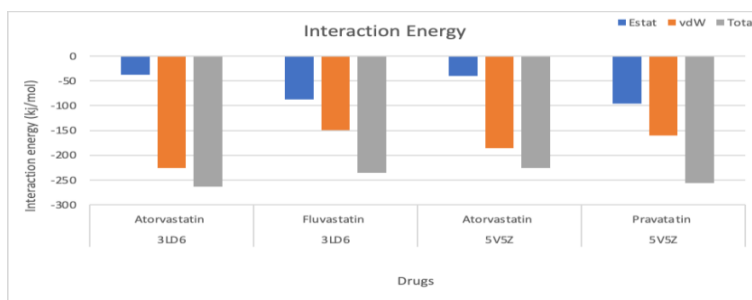


Figure (16): Graph showing Interaction energy between the ligand and the target protein (3LD6 and 5V5Z) of statin drugs

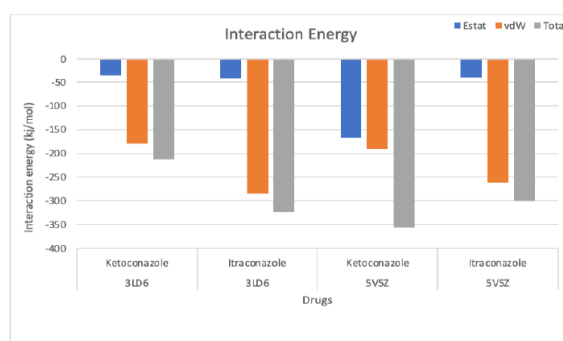


Figure (17) : Graph showing Interaction energy between the ligand and the target protein (3LD6 and 5V5Z) of standard drugs

4.1.4. Center of mass(COM) distance

A plot is created by calculating the COM-COM distance between the heavy atoms of the protein binding site residues surrounding the ligand.

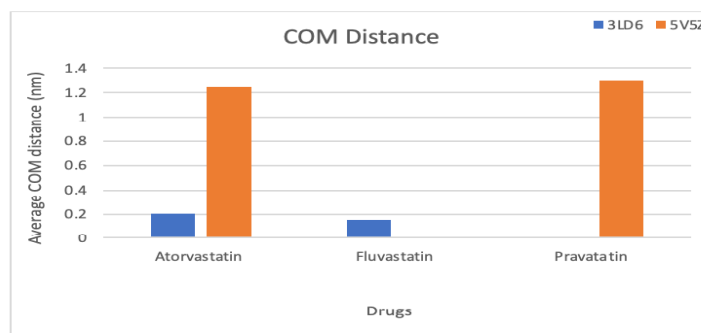


Figure (17): Graph showing the centre of mass values between the ligand and the target protein (3LD6 and 5V5Z) of statin drugs

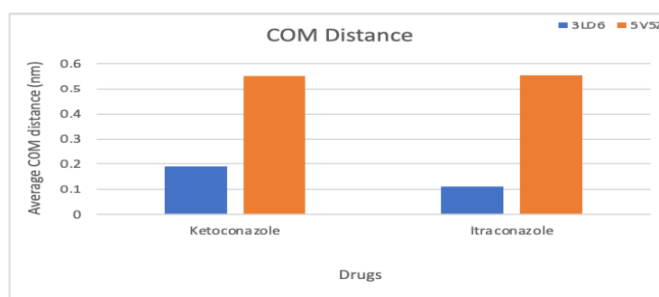


Figure (18): Graph showing the centre of mass values between the ligand and the target protein (3LD6 and 5V5Z) of standard drugs

4.2. Invitro studies

The antifungal activity of all three extracts was evaluated against the pathogenic microbes, The *Microsporum Canis*, *Trichophyton rubrum*, *Epidermophyton floccosum* activity was evaluated by the method of disk diffusion. The antifungal sensitivity test was performed to determine the given sample's sensitivity towards the given sample atorvastatin shows the zone of inhibition against *Microsporum canis*, *Trichophyton rubrum* and *Epidermatophyton floccosum* tested against three concentrations the zone of inhibition shown by the concentration [9]. The results are summarized in Table 4. A clear zone of inhibition was observed by disc diffusion method by against all three fungal species viz. *Epidermatophyton floccosum*, *Trichophyton rubrum*, and *Microsporum canis* as were observed in figures 18, 19 and 20 respectively.

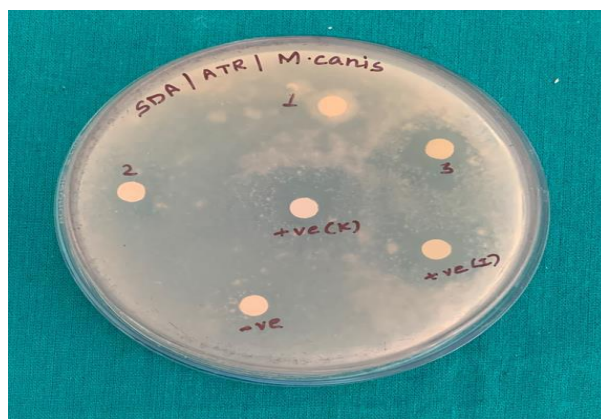


Figure (19) : Zone of Inhibition of drugs against *Microsporum Canis*



Figure (20) : Zone of Inhibition of drugs against *Trichophyton rubrum*



Figure (21) : Zone of Inhibition of drugs against *Epidermatophyton floccosum*

4.2.1. Minimum Inhibitory Concentration

The antifungal sensitivity test was performed to determine the given sample's sensitivity towards the given sample atorvastatin shows the zone of inhibition against three fungal strain *Trichophyton rubrum*, *Epidermatophyton. floccosum* & *Microsporum canis* tested against three concentrations of atorvastatin the zone

of inhibition summarized shown in figure 19, 20 & 21 .

Table (5): Summary of Minimum Inhibitory concentration of Atorvastatin against three fungal strains

Sample	Fungal strains	Concentration of MIC Value ($\mu\text{g/ml}$)
Atorvastatin	Trichophyton rubrum	150 $\mu\text{g/ml}$
	Microsporum canis	125 $\mu\text{g/ml}$
	Epidermatophyton floccosum	150 $\mu\text{g/ml}$
Itraconazole	Trichophyton rubrum	25 $\mu\text{g/ml}$
	Microsporum canis	25 $\mu\text{g/ml}$
	Epidermatophyton floccosum	12.5 $\mu\text{g/ml}$
Ketoconazole	Trichophyton rubrum	25 $\mu\text{g/ml}$
	Microsporum canis	25 $\mu\text{g/ml}$
	Epidermatophyton floccosum	25 $\mu\text{g/ml}$

The minimum inhibitory concentration value for atorvastatin as found against fungal strain Microsporum canis was 125 $\mu\text{g/ml}$ for atorvastatin & ketoconazole & Itraconazole 25 $\mu\text{g/ml}$ respectively. Trichophyton rubrum 75 $\mu\text{g/ml}$ & ketoconazole 25 $\mu\text{g/ml}$, 50 $\mu\text{g/ml}$ respectively. Epidermatophyton floccosum for atorvastatin 150 $\mu\text{g/ml}$ & ketoconazole 25 $\mu\text{g/ml}$ & Itraconazole 12.5 $\mu\text{g/ml}$ shown in table 5.

5. Conclusion & discussion

An ideal antifungal agent should have minimal effect on human CYP51 enzymes while keeping potent inhibition of fungal enzyme to reduce the side effects for better clarification and comparison of the selectivity of compounds on fungal versus human enzyme docking was performed on both Fungal CYP51 and human CYP51 enzymes.

Acknowledgments

The authors express their gratitude to the Hon. Founder President of Amity University Uttar Pradesh, Dr. Ashok K. Chauhan, and the Amity Institute of Pharmacy, Lucknow campus, for providing the necessary facilities for the authors to write this chapter. Sudip Roy, Aiswarya Pawar, and Mahima Kori deserve special recognition for their help in refining the docking methods and for using the computational resources that were essential to this effort.

References

- [1] Ramdhani, D., & Mustarichie, R. (2020). Molecular Docking Studies of Epifriedelanol from GuazumaUlmifolia as a Natural Antihyperlipidemic Agents.
- [2] Khan, A., Sharma, S., Gehlot, A., Gupta, M., & Alam, M. (2020). Antifungal screening and molecular docking simulation of silica supported synthesized sitosteryl hydrogen phthalate using microwave irradiation. HemijskaIndustrija, 74(6), 377–388.
- [3] Paul Andrei & Georgeta (2021). Coumarin derivatives with potential antimicrobial activity insilico studies. AnaleleUniversității din Oradea-Fascicula Chimie, Vol. XXVIII(28).
- [4] Ye, L., Lin, P., Du, W., Wang, Y., Tang, C., & Shen, Z. (2018). Preparation, Antidermatophyte Activity, and Mechanism of Methyl phloroglucinol Derivatives. Frontiers in Microbiology, 9, 2262.
- [5] Scorzoni L, de Paula e Silva AC, Marcos CM, Assato PA, de Melo WC, de Oliveira HC, Costa-Orlandi CB, Mendes-Giannini MJ, Fusco-Almeida AM. Antifungal therapy: new advances in the understanding and treatment of mycosis. Frontiers in microbiology. 2017 Jan 23; 8:36.
- [6] Nigam PK. Antifungal drugs and resistance: Current concepts. Our Dermatology Online. 2015 Apr 1;6(2):212.
- [7] Fisher MC, Hawkins NJ, Sanglard D, Gurr SJ. Worldwide emergence of resistance to antifungal drugs challenges human health and food security. Science. 2018 May 18;360(6390):739-42.
- [8] Cowen LE, Sanglard D, Howard SJ, Rogers PD, Perlín DS. Mechanisms of antifungal drug resistance. Cold Spring Harbor perspectives in medicine. 2015 Jul 1;5(7):a019752.
- [9] Denning DW, Bromley MJ. How to bolster the antifungal pipeline. Science. 2015 Mar 27;347(6229):1414-6.
- [10] Nigam PK. Antifungal drugs and resistance: Current concepts. Our Dermatology Online. 2015 Apr 1;6(2):212
- [11] Mast N, Zheng W, Stout CD, Pikuleva IA. Antifungal azoles: structural insights into undesired tight binding to cholesterol-metabolizing CYP46A1. Molecular Pharmacology. 2013 Jul 1;84(1):86-94.
- [12] White TC, Findley K, Dawson TL, Scheynius A, Boekhout T, Cuomo CA, Xu J, Saunders CW. Fungi on the skin: dermatophytes and Malassezia. Cold spring harbor perspectives in medicine. 2014 Aug 1;4(8): 019802.

- [13] Dudley JT, Deshpande T, Butte AJ. Exploiting drug–disease relationships for computational drug repositioning. *Briefings in bioinformatics*. 2011 Jul 1;12(4):303-11.
- [14] Arnold TM, Dotson E, Sarosi GA, Hage CA. Traditional and emerging antifungal therapies. *Proceedings of the American Thoracic Society*. 2010 May 15;7(3):222-8.
- [15] Ostrosky-Zeichner L, Casadevall A, Galgiani JN, Odds FC, Rex JH. An insight into the antifungal pipeline: selected new molecules and beyond. *Nature reviews Drug discovery*. 2010 Sep;9(9):719-27.
- [16] Sangamwar AT, Deshpande UD, Pekamwar SS. Antifungals: need to search for a new molecular target. *Indian journal of pharmaceutical sciences*. 2008 Jul;70(4):423.
- [17] Nucci M, Perfect JR. When primary antifungal therapy fails. *Clinical infectious diseases*. 2008 May 1;46(9):1426-33.
- [18] Georgopapadakou NH, Walsh TJ. Antifungal agents: chemotherapeutic targets and immunologic strategies. *Antimicrobial agents and chemotherapy*. 1996 Feb;40(2):279-91.
- [19] Khurana A, Sardana K, Chowdhary A. Antifungal resistance in dermatophytes: Recent trends and therapeutic implications. *Fungal Genetics and Biology*. 2019 Nov 1; 132:103255.
- [20] Hokken MW, Zwaan BJ, Melchers WJ, Verweij PE. Facilitators of adaptation and antifungal resistance mechanisms in clinically relevant fungi. *Fungal genetics and Biology*. 2019 Nov 1;